Visualization and Processing of Mesospheric Hydroxyl Infrared Emissions from SABER

Kenneth B. Reese
Department of Electrical and Computer Engineering
Utah State University
4140 Old Main Hill
Logan, UT 84322-4140

ABSTRACT

The SABER (Sounding of the Atmosphere using Broadband Emission Radiometry) instrument on NASA's TIMED (Thermosphere Ionosphere Mesosphere Energetics and Dynamics) satellite is a 10-channel infrared radiometer that has been collecting data about Earth's upper atmosphere for over three years. Two radiometric channels of SABER are centered at wavelengths of 1.67 and 2.06 μm, corresponding to OH ($\Delta v = 2$) emissions derived from Meinel rotation-vibration emission bands. The purpose of this study is to develop algorithms to accurately process and display SABER data. Various interpolation methods were investigated and tested to precisely interpolate recorded data points globally. Global airglow volume emission rate (VER) maps were developed.

I. INTRODUCTION

The Mesosphere-Lower Thermosphere (MLT) region of the Earth's atmosphere has traditionally been the least explored and understood of all atmospheric regions. Central to this region is the mesopause, defined as "the altitude of the temperature minimum between the stratopause (40 – 50 km) and the lower thermosphere (above 100 km)" [1].

A study of the MLT region is imperative to an overall understanding of how the atmosphere changes globally due to human effects and differences in solar cycles. This region is the transition area from Earth's environment to that of space in temperature and physical and chemical processes. It is in the MLT region that photolysis, the splitting of a molecule into more elementary parts due to the absorption of a photon of the sun's energy, first occurs.

Of interest in this study is the infrared emission from the hydration of ozone due to photolysis, $H + O_3 \rightarrow OH^{\ddagger} + O_2$. The incoming photon from the sun strips off one of the oxygen atoms from the O_3 molecule and creates an excited hydroxyl molecule and an O_2 molecule. Sixty percent of the mesospheric energy from this exothermic reaction is released as heat, while forty percent is released as infrared airglow [2].

Historically, several factors have constrained global observations of the infrared OH airglow. First, ground-based instruments can only observe a small portion of the Earth's atmosphere at a specific latitude and longitude. Additionally, measurements of the MLT region by ground instruments are filtered and skewed by the absorption and scattering of the lower atmospheric regions. Sounding rockets have been used to launch instruments up into the MLT region for altitude distribution measurements, but again this yields results at only one location on the Earth for a very brief period of time. The region is also too

high to be reached by aircraft and balloon-borne sensors.

II. TIMED Mission

For scientists to better understand and model the Earth's upper atmosphere, the need arose for a comprehensive, satellite-based global study of the MLT region. The Thermosphere Ionosphere Mesosphere Energetics and Dynamics (TIMED) spacecraft was designed as part of NASA's Solar Terrestrial Probes (STP) Program to address this objective.

The TIMED satellite was designed and built by NASA and The Johns Hopkins University Applied Physics Laboratory. It was launched December 7, 2001 aboard a Delta II 7920-10 rocket from the Vandenberg Air Force Base, CA. The TIMED spacecraft observes various aspects of the MLT region from its 625-km circular orbit using four principal instruments: GUVI (Global Ultraviolet Imager), SEE (Solar Extreme Ultraviolet Experiment), TIDI (TIMED Doppler Interferometer), and SABER (Sounding of the Atmosphere using Broadband Emission Radiometry).

III. SABER Sensor

The SABER sensor is a 10-channel infrared radiometer that was designed to measure various seasonal, latitudinal, and temporal variations in the MLT region from 60-180 km [3]. SABER measures the infrared radiation from the atmosphere over a broad spectral range and detects sources of atmospheric cooling, including the airglow, which occurs when energy is radiated back into space in the form of light [4]. An important contributor to the atmospheric airglow in the mesopause region is the vibrationally-excited OH (hydroxyl) radical. Although this radical is a minor species in the mesosphere, it plays a critical role in the chemistry of the MLT region as it is chemically very active [5].

Channels eight and nine of SABER have optical bandpasses centered at wavelengths of 2.06 and 1.67 μm respectively, corresponding to OH ($\Delta v = 2$) emissions derived from Meinel vibration-rotation sequence. An overlay of the channels' optical filter bandpass responses with the OH Meinel spectrum is displayed in fig. 1.

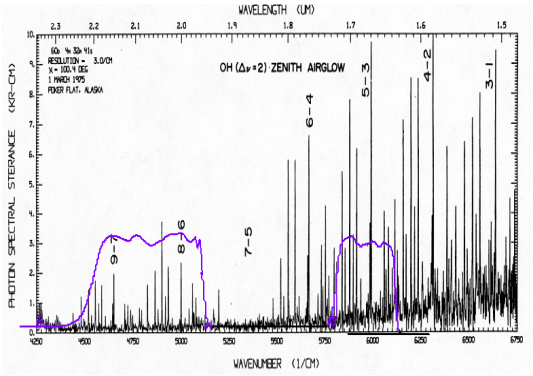

Fig. 1: The OH Meinel spectrum overlaid with the optical filter bandpasses of SABER channels eight (left) and nine (right).

SABER collects three-dimensional data about the OH airglow in the MLT region through the satellite motion and a rocking mirror which performs a limb scan at a tangent point roughly 2700 km from the satellite as shown in fig. 1.4. As the viewing field scans from 130 km down to 60 km and back up again, the sensor looks through different layers of the Earth's airglow. Each scan lasts for a time duration of approximately 6.98 seconds. Since the satellite is moving in orbit and the Earth is rotating under it during a scan, consecutive scans are separated in latitude by approximately 1.5°. Because of the spacecraft's highly inclined orbit of 74.1°, the longitudinal separation between scans varies greatly depending upon latitude. At high latitudes, separation in longitude can be as much as 6°. Additionally, as the spacecraft orbits, each ground path is

separated by approximately 2,725 km, or 24° longitude.

SABER telemetry data are downlinked to the Mission Data Center of the NASA Langley Research Center. Different levels of processing of the raw data are performed by G & A Technical Software (GATS), Hampton, Virginia. The level 2A data that were used in this project were downloaded from the SABER FTP site as daily NetCDF files [6].

IV. KRIGING INTERPOLATION

The issue of how to best interpolate SABER data points was explored in order to display the OH airglow effectively. The interpolation method sought needs to give the most accurate reflection of 3-D global OH distribution in the MLT region. The goal of this study was to find a method that achieves prime visualization and computation time while minimizing error.

Various interpolation methods were tested with numerous test patterns and SABER data. The details of such testing will not be discussed in this paper; only the conclusion that the Kriging hybrid method yielded the best visualization of the methods tested on both the test patterns and SABER data. Kriging produced the lowest mean-square error and standard deviation from the test patterns.

Kriging is an interpolation method that was developed by D. G. Krige, a professor at the University of Witwatersrand, South Africa, in the 1950s originally for use in geostatistics [7]. Today Kriging has found use in many areas outside of geostatistics, being used here in atmospheric modeling. This method incorporates both regression and correlation models of the entire sampled data set in predicting unmeasured points. It takes into account both the distance between measurement data points and the grid sites to be calculated, as well as how close the measured points are to each other to form a spatial relationship matrix. It takes advantage of the random variable nature of spatial measurements to generate a more accurate estimate of a field of values. Additionally, the Kriging technique provides a measure of the accuracy of its measurements since it takes into account the statistical relationship between measured points. With a method of calculating the mean-square error, the Kriging algorithm can attempt to optimize the interpolation through iterations based upon minimizing the error model [8].

The stochastic process model that is used to generate the correlation parameters should reflect as closely as possible the characteristics of the given data. For instance, data recording events of a parabolic behavior near the origin should be modeled by a Gaussian, cubic, or spline correlator. In the case of SABER, the OH VER data collected exhibit a linear behavior near the origin; thus an exponential correlator was used. Mathematically, the correlation between two points x and w on the grid space is given by

$$P(\theta, w, x) = \prod_{j=1}^{n} \exp(-\theta_j \left| d_j \right|); \qquad (3.1)$$

where n is the dimension of the input spatial matrix (2 in the case of two-dimensional SABER displays), d_j is the distance between the jth element of w and x, and θ_j is the correlation parameter. The data are assumed to be isotropic; i.e., the correlations between data points are the same in all directions.

The two-dimensional Kriging algorithm used to interpolate SABER data receives as its input an m × 3 data matrix, where m is the number of recorded data points. The first two columns of this matrix contain the latitude and longitude values, respectively, of the measured OH

VER tangent points. The third column of the data matrix contains the measured VER value corresponding to each latitude/longitude point. Throughout this discussion of the Kriging algorithm, notation used by Lophaven, Nielsen, and Sondergaard [8], [9] was adopted and used when possible. Thus the notation S is used to represent a matrix containing the first two columns of the data matrix, and Y to represent a vector containing the third column of VER values in the data matrix. S and Y are normalized by subtracting each columnar element by the mean of the entire vector and then dividing this difference by the standard deviation of the vector.

The next step in the Kriging algorithm is to form a matrix D of size $(m*(m-1))/2 \times 3$ which contains the distances between measured points. This matrix is used to verify that the same point in S (up to the precision of the processor) is not duplicated, cause inconsistencies in measured data. D will also be used later in conjunction with (3.1) to determine the statistical correlation between measured points.

A regression model must be formed in Kriging so that each Kriging predictor $\hat{y}$ of the deterministic response y(x) can be fully characterized. In the case of using SABER data, a simple polynomial regression of first order (linear regression) was used since this approach most accurately models the physical distribution of OH airglow in the MLT region as experimentally obtained from sounding rocket experiments [10]. The regression polynomials f(x) therefore are

$$f_1(x) = 1, \quad f_2(x) = x_1, \quad f_3(x) = x_2. \tag{3.2}$$

The $m \times 3$ regression matrix F is formed as a linear combination of the basis functions f_1, f_2, and f_3 by $F_{i,j} = f_j(s_i)$,

$$F = \begin{bmatrix} f_1(s_1) & f_2(s_1) & f_3(s_1) \\ f_1(s_2) & f_2(s_2) & f_3(s_2) \\ \vdots & \vdots & \vdots \\ f_1(s_m) & f_2(s_m) & f_3(s_m) \end{bmatrix}. \tag{3.3}$$

Kriging predictors at each desired point can now be modeled as a realization of the regression model in (3.3) and the random process on (3.1). The exact model used will be discussed after additional needed parameters are defined.

The Kriging predictors are modeled as a realization of stochastic process in (3.1) through the correlation matrix R. R is an $m \times m$ matrix containing the random process correlations between measured points in S,

$$R = \begin{bmatrix} P(\theta, s_1, s_1) & P(\theta, s_1, s_2) & \dots & P(\theta, s_1, s_m) \\ P(\theta, s_2, s_1) & P(\theta, s_2, s_2) & \dots & P(\theta, s_2, s_m) \\ \vdots & \vdots & \ddots & \vdots \\ P(\theta, s_m, s_1) & P(\theta, s_m, s_2) & \cdots & P(\theta, s_m, s_m) \end{bmatrix}, \tag{3.4}$$

where $P(\theta, s_i, s_j)$ is defined in (3.1). The function r(x) is also defined at some desired, but unknown point x as

$$r(x) = \left[P(\theta, s_1, x) \quad \cdots \quad P(\theta, s_m, x) \right]^T. \tag{3.5}$$

R is a function of θ, which is defined as the correlation parameter. The optimal choice of θ, known as the maximum likelihood estimator (MLE), is that θ which minimizes the equation

$$\psi(\theta) = \left| R(\theta) \right|^{\frac{1}{m}} \cdot \sigma^2(\theta). \tag{3.6}$$

This MLE θ is determined by an iterative process of evaluating (3.6) with various values of θ within a given bound until a global minimum is reached.

Evaluation of (3.6) must be performed with caution as the process could be a computationally intensive task and the determinant of R could possibly yield erroneous values if R is ill-conditioned. To avoid these potential problems and increase efficiency, the Cholesky factorization of R is calculated with the MATLAB command `C = chol(R)`. It is assumed at this point that R is symmetric positive definite so that the Cholesky factorization can be computed. The lower triangle of C is used by taking the transpose of the C output from the `chol` command. Now let

$$\widetilde{F} = C^{-1}F, \tag{3.7}$$

where F is defined in (3.3). Taking the QR factorization of (assuming it is not too ill-conditioned) yields

$$\widetilde{F} = QG^T, \tag{3.8}$$

where Q is an m × 3 matrix with orthonormal columns and GT is a 3 × 3 upper triangular matrix. With these matrices calculated, the following definitions can be adopted:

$$\widetilde{Y} = C^{-1}Y, \tag{3.9}$$

$$\beta = G^T(Q^T\widetilde{Y}), \tag{3.10}$$

$$\rho = \widetilde{Y} - \widetilde{F}\beta, \tag{3.11}$$

$$\gamma = \rho^{-T}C, \tag{3.12}$$

$$\sigma^2 = \frac{\sum_{i=0}^{m-1}\rho_i^2}{m}, \tag{3.13}$$

where β is the 3 × 1 generalized least squares solution to the regression problem with respect to R, and σ^2 is the variance estimate. The m × 1 matrix γ contains correlation constants between the samples.

The Kriging predictor ŷ at any unknown point x can now be calculated as

$$\hat{y}(x) = f(x)^T\beta + r(x)^T\gamma. \tag{3.14}$$

Note that for any given day's worth of SABER data, β and γ are constants. Thus for every new desired point x to be calculated, the predictor ŷ can be found by simply computing the 3 × 1 vector f(x) and the m × 1 vector r(x). Note also that the ŷ in (3.14) is the scaled predictor since S and Y were normalized as the first step in the Kriging algorithm. To un-normalize the predictor, simply multiply ŷ by the x and y coordinate scale factors.

It can be seen that the variance estimate σ^2 was calculated in (3.13), but not used in the calculation of the predictor in (3.14). This variance estimate was calculated so that it can be used in the calculation of the mean-square error (MSE) of the predictor. The MSE is defined as

$$\varphi(x) = E\left[(\hat{y}(x) - y(x))^2\right]. \tag{3.15}$$

Building upon the fact that σ^2 has already been calculated, to solve for the MSE we can define

$$\widetilde{r} = C^{-1}r(x), \tag{3.16}$$

$$v = G^{-1}(\widetilde{F}\widetilde{r} - f(x)), \tag{3.17}$$

where C is defined as the lower triangle of the Cholesky factorization of R, r(x) is defined in (3.5), G is defined in (3.8), is defined in (3.7), and f(x) is defined in (3.2). The MSE can now more efficiently be solved as

$$\varphi(x) = \sigma^2(1 + \|v\|^2 - \|\tilde{r}\|^2). \qquad (3.18)$$

While Kriging interpolation yields more accurate models of global OH VER distribution when applied to SABER data, the number of measured data points for even a single day of TIMED orbits makes using the Kriging algorithm by itself cumbersome and computationally impractical. The spatial resolution of the resulting global map is limited because of the large memory requirements and computation time involved in Kriging to an area larger than 100 square data points.

Because of these challenges in using Kriging, the `SABER_Krig` function was developed for the processing of SABER data which uses a hybrid Kriging/Cubic spline approach. Refer to the Kriging hybrid source code provided at http://spacegrant.usu.edu/research.html for MATLAB implementation of the algorithm. The initial interpolation of the data is performed by straight Kriging to an area of less than 100×100 data points. This block of data is then refined to a default size of 480×640 using MATLAB's built-in cubic interpolation that is part of the `griddata` function. The dimension of the Kriging block, the final width, and the final height each can be easily changed as input parameters to the function. The resulting plot has the accuracy of Kriging, but with a higher resolution and a much shorter computation time.

Figure 2 displays the data points of the peak volume emission rate (VER) of each SABER scan event on March 21, 2002. This data was projected onto a two-dimensional map with a Mercator projection to be interpolated. The color of each data point correlates to the value of the peak VER at that geographical location. Figure 3 illustrates the result of interpolating the data points of fig. 2 with a Kriging/Cubic hybrid method. In the testing of various interpolation methods, Kriging resulted in the lowest mean-square error and most accurate visualization of all tested methods. Figure 4 presents the interpolation of the same data points of fig. 2 with a Kriging/Cubic hybrid, but uses the altitude of the peak VER as the given data values to interpolate. Figure 5 displays a `meshgrid` plot of the Kriging hybrid interpolation of the peak VER data points for March 21, 2002. The measured data points from SABER are also displayed as black points. It can be seen that since in the Kriging algorithm each given data point is represented by a regression polynomial and a random variable, it does not interpolate to the exact measured value at all given points. It assumes that there could be possible error in the measured value itself, and interpolates based on the prediction surface established from the complete set of observational data.

It is also desirable in the analysis of SABER data to interpolate over a three-dimensional volume of latitude, longitude, and altitude. Whereas in the previous discussion nighttime OH VER values were taken only at the altitude of the peak intensity value, in a three-dimensional interpolation an altitude profile is established together with the latitude and

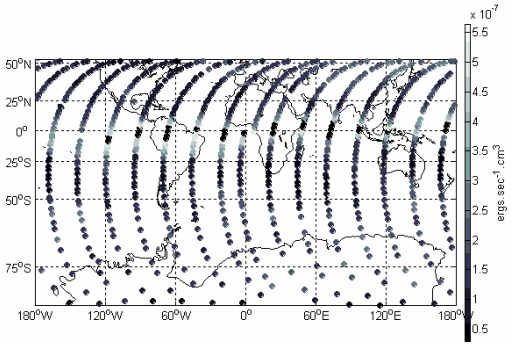

Fig. 2: Mercator projection of nighttime SABER scan events on March 21, 2002. The color of each marker represents the peak volume emission rate value of its associated scan.

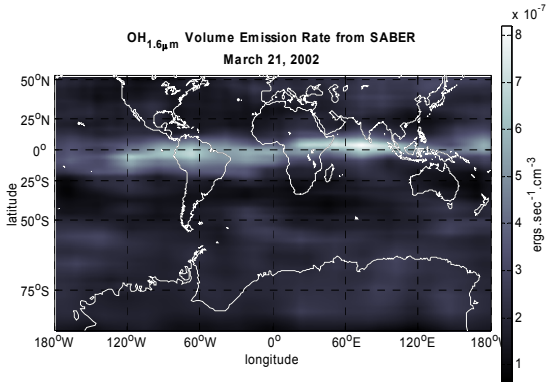

Fig. 3: Peak nighttime OH 1.6-µm volume emission rate on March 21, 2002. Data were interpolated with a Kriging/Cubic hybrid.

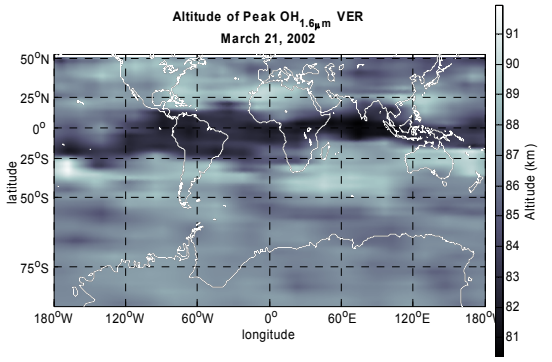

Fig. 4: Altitude of peak nighttime OH 1.6-µm volume emission rate on March 21, 2002. Data were interpolated with a Kriging/Cubic hybrid.

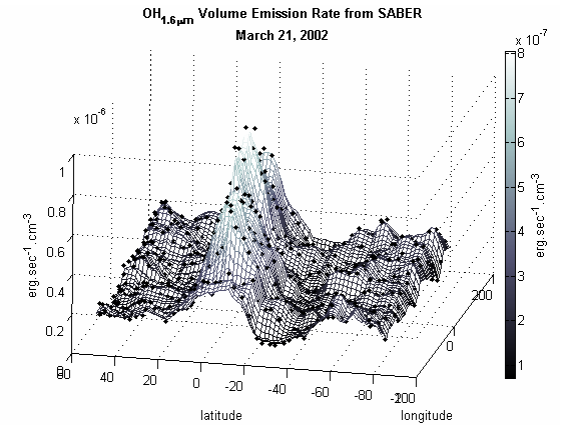

Fig. 5: MATLAB meshgrid plot of peak nighttime OH 1.6-µm volume emission rate on March 21, 2002. Measured data points are represented by black dots and were interpolated with a Kriging/Cubic hybrid.

longitude profiles. The Kriging algorithm can be modified to accommodate higher-dimensional interpolation. In the three-dimensional case, the dimension of the input spatial matrix is n = 3. An input data matrix of size m × 4 is then formulated where m is the number of sampled points. The first three columns are latitude, longitude, and altitude, respectively, (comprising the S matrix), and the fourth column still contains the VER values for each associated point in the three-dimensional volume (comprising the Y vector).

Performing a three-dimensional Kriging hybrid interpolation on the nighttime OH 1.6-µm data from March 21, 2002, and then plotting the isosurface of four different emission levels yields the plot of fig. 6. The added benefit of altitude profiling is manifest in this plot. It can be seen that peak emissions occur at the equator (0° latitude) as expected, and that these emissions do indeed occur at lower altitudes than at other parts of the globe. It should be noted that Kriging is an order $O(n^2)$ operation; thus an additional dimension of interpolation significantly increases the computation time and required computer memory to complete the Kriging algorithm.

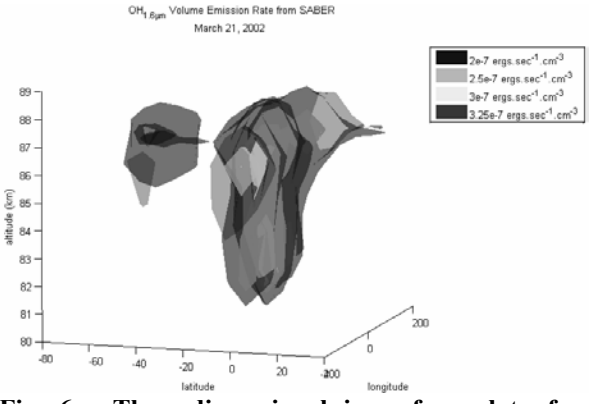

Fig. 6: Three-dimensional isosurface plot of peak nighttime OH 1.6-µm volume emission rate on March 21, 2002. Interpolation was performed with a three-dimensional Kriging/Cubic hybrid.

V. CONCLUSIONS

The TIMED mission in general has been a success for NASA and has met or exceeded its scientific goals. Its four instruments, including SABER, have retrieved invaluable data which has improved and validated models for the MLT region of Earth's atmosphere. SABER has enabled scientists to study global and seasonal trends of the fundamental processes governing the energetics, chemistry, and dynamics of the atmospheric region extending from 60 km to 180 km.

This presentation covers the development of the Kriging interpolation algorithm used to accurately display the findings of the SABER mission. Maps of the global distribution of nighttime airglow were developed for two SABER infrared optical bands centered at wavelengths of 1.67 and 2.06 μm. It was found that to overcome the difficulties of interpolating between measured tangent points along the satellite ground path, of the methods tested, a Kriging hybrid algorithm yields the best visualization with the smallest mean-square error. Test patterns were developed to verify this conclusion by comparison with the other methods.

REFERENCES

[1] K. Smith, "Physics and chemistry of the mesopause region," *Journal of Atmospheric and Solar-Terrestrial Physics,* vol. 66, pp. 839-857, 2004.

[2] R. Fielding, "*Satellite-based investigation of mesospheric infrared emissions*," Utah State University, Logan, Utah, 2005.

[3] Space Dynamics Laboratory, "SABER preliminary design review," Utah State University, Logan, Utah, SDL/96-067, Dec. 1996.

[4] Johns Hopkins University, Applied Physics Laboratory, "TIMED fact sheet," [Online]. Available: http://www.timed.jhuapl.edu/press2/timed_factsheet.pdf.

[5] D. J. Baker, "The Upper-Atmospheric Hydroxyl Airglow," Air Force Geophysics Laboratory, Hanscom Air Force Base, MA, May, 1976.

[6] G & A Technical Software, "Level 2A software development document for SABER," GATS, Hampton, VA, GATS Doc No: SABER-L1BSDD-98-1.V1.

[7] D.G. Krige, "A statistical approach to some basic mine valuation problems on the Witwatersrand," *Journal of the Chemical, Metallurgical, and Mining Society of South Africa,* vol. 52, pp. 119-139, Dec. 1951.

[8] S. N. Lophaven, H. B. Nielsen, J. Sondergaard, "DACE—A MATLAB Kriging Toolbox, Version 2.0," Technical University of Denmark, Lyngby, Denmark, Tech. Rep. IMM-TR-2002-12, August 1, 2002.

[9] S. N. Lophaven, H. B. Nielsen, J. Sondergaard, "Aspects of the MATLAB Toolbox DACE," Technical University of Denmark, Lyngby, Denmark, Tech. Rep. IMM-REP-2002-13, 2002.

[10] D.J. Baker and A.T. Stair Jr., "Rocket measurements of the altitude distribution of the hydroxyl airglow," *6th International Symposium on Solar Terrestrial Physics,* Part II, Toulouse, France, June 30 – July 5, 1986.